

Analysis of the interaction between Myo5 and OSB proteins and its possible role in endocytosis

TREBALL DE FINAL DE GRAU

Grau de Biotecnologia

5th September 2016

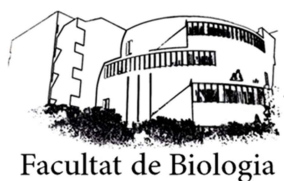
Aina Abad Lázaro

The endocytic pathway and the actin cytoskeleton, IBMB, CSIC

Tutors:

María Isabel Geli Fernández-Peñaflor

Joan Carles Ferrer Artigas



UNIVERSITAT DE
BARCELONA



Abstract

The oxysterol-binding proteins (OSBP) constitute an evolutionary conserved family implicated in establishing contact sites between the endoplasmic reticulum and diverse cellular membranes. Those contacts have been involved in regulating calcium signalling, the vesicular trafficking, the lipid metabolism, and the nonvesicular sterol transfer. In yeast, there are 4 OSBP (Osh2, Osh3, Osh6 and Osh7), that specifically connect the cortical ER with the plasma membrane. Divergent N-terminal domains suggest that these proteins might fulfil specialized functions, but this issue has not been addressed. In the present work we demonstrate using the Two Hybrid assay and co-immunoprecipitation experiments that Osh2 specifically interacts with the endocytic type I myosin Myo5, which plays an essential function initiating actin polymerization at endocytic sites. Further, we found that the interaction is mediated by the SH3 domain of Myo5 and most likely a PPPVP motif located immediately upstream of the OSBP-related sterol-binding domain (ORD) of Osh2. In addition, we detect a weaker interaction with Osh3, which is mediated by a different Myo5 domain. Osh2 binds to the yeast VAP (vesicle-associated membrane protein-associated proteins) homologues Scs2/Scs22 through their FFAT motif. We hypothesized that Osh2 and maybe Osh3 bridge the interaction of Myo5 to the VAPs to establish an ER/endocytic site contact site probably involved in vesicle scission.

INDEX

1. INTRODUCTION.....	1
1.1. <i>SACCHAROMYCES CEREVISIAE</i> AS A MODEL ORGANISM.....	1
1.2. ENDOCYTOSIS	1
1.3. TYPE I MYOSINS.....	3
1.4. OXYSTEROL BINDING PROTEINS	4
1.5. ENDOPLASMIC RETICULUM / PLASMA MEMBRANE CONTACT SITES.....	6
2. PRELIMINARY RESULTS AND OBJECTIVES.....	8
3. MATERIALS AND METHODS	10
3.1. PLASMIDS	10
3.2. POLYMERASE CHAIN REACTION.....	10
3.3. YEAST CULTURE, TRANSFORMATION AND STRAINS	11
3.4. PROTEIN EXTRACTIONS	13
3.5. SODIUM DODECYL SULFATE - POLYACRYLAMIDE GEL ELECTROPHORESIS.....	14
3.6. IMMUNOBLOT.....	14
3.7. IMMUNOPRECIPITATION (IP) AND CO-IMMUNOPRECIPITATION (CO-IP).....	15
3.8. TWO HYBRID	17
4. RESULTS.....	18
4.1. MYO5 INTERACTS WITH OSH2 AND OSH3 IN A TWO HYBRID ASSAY	18
4.2. MYO5 INTERACTS WITH OSH2 AND OSH3 USING DIFFERENT DOMAINS	19
4.3. THE INTERACTION OF MYO5 AND OSH2 PROBABLY INVOLVES A POLYPROLINE MOTIF IN OSH2. 20	21 21
4.4. ANALYSIS OF THE INTERACTION BETWEEN MYO5 AND ORPs BY CO- IMMUNOPRECIPITATION.....	21 21
5. DISCUSSION	23
5.1. MYO5 INTERACTS WITH OSH2 AND PROBABLY OSH3.....	23
5.2. OSH2 AND OSH3 INTERACT WITH THE SH3 AND TH1/TH2 DOMAINS OF MYO5, RESPECTIVELY.....	24 24
6. CONCLUSIONS AND FUTURE LINES.....	26
7. REFERENCES.....	28

1. Introduction

1.1. *Saccharomyces cerevisiae* as a model organism

Saccharomyces cerevisiae is the yeast species that has been the most intensively studied eukaryotic model organism in molecular and cell biology, much like *Escherichia coli* as the model bacterium. *S. cerevisiae* has several upsides compared to other model organisms: its generation time is quite short (1,5 h at 30°C), can enter meiosis and therefore, it can be used for sexual genetics research, can easily be genome edited by homologous recombination, and last, but perhaps most important it shares most of the physiological mechanisms with superior eukaryotes, with most of its proteins being highly conserved across evolution (Drubin et al. 1988).

1.2. Endocytosis

Endocytosis is the process whereby eukaryotic cells internalize plasma membrane (PM) – associated surface molecules such as signalling receptors, channels and lipids, together with extracellular material.

At the cellular level, endocytosis is required for nutrient uptake (Kumari et al. 2010), and controls the PM protein composition thereby playing essential regulatory roles in cell signalling, the establishment of cell polarity (Scita & Di Fiore 2010 and Lecuit & Pilot 2003), cell division and cell motility. Therefore, endocytosis fundamentally supports cellular physiology and homeostasis.

Clathrin-mediated endocytosis (CME) is the best characterized of all the endocytic pathways. During CME, the PM invaginates into the cell, forming a vesicle whose content is called cargo. Cargo destined for internalization is delivered to early endosomal compartments, from where it can either be recycled back to the plasma membrane or other cellular organelles or be transported to the late endosomal and lysosomal compartments for degradation.

This process requires the ordered recruitment of endocytic proteins to the plasma membrane, which include cargo adaptors; clathrin, BAR domain containing proteins and actin cytoskeletal proteins (Engqvist-Goldstein & Drubin 2003 and Merrifield 2004) (Figure 1).

The dynamics of coat assembly (early and immobile stage), membrane invagination (mid and slow mobile stage), vesicle scission and vesicle inward movement (late and fast mobile stages) are largely conserved across evolution (Boettner et al. 2012, McMahon & Boucrot 2011, Taylor et al. 2011 and Weinberg & Drubin 2012), and in many cases, protein homologues are responsible for carrying out the same steps (Figure 1).

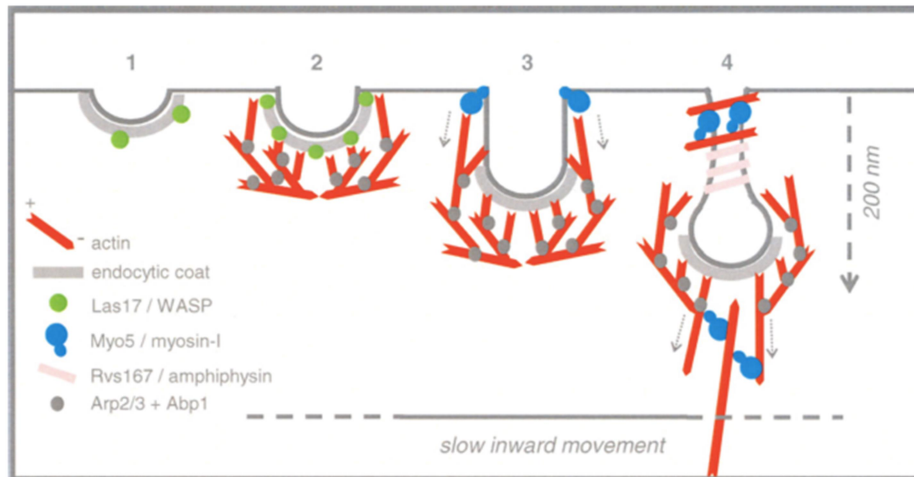


Figure 1. Molecular model for CME. Endocytic uptake in yeast can be dissected into the following steps: (1) assembly of an hemispherical clathrin coat previous to massive actin polymerization, (2) Arp2/3-dependent formation of an actin network on the surface of the endocytic coat induced by Las17/WASP and Pan1, (3) elongation of the incipient invagination powered by Myo5/myosin-I-induced actin polymerization at the base of the profile and by the mechanochemical activity mediated by the myosin, (4) formation of two acto-myosin structures that cooperate with the yeast amphiphysins (Rvs167) in the fission event by generating tension along the endocytic profile (Girao et al. 2008).

Vesicles are coated with clathrin, whose basic subunit is a triskelion: a trimer of clathrin heavy chains, each with an associated clathrin light chain. The controlled formation of a dense and branched actin-filament network provides forces critical for driving subsequent membrane tubulation and vesicle scission (Engqvist-Goldstein & Drubin 2003). Arp2/3 is the complex responsible for the nucleation of these actin patches, and this event coincides with endocytic membrane invagination and vesicle scission (Idrissi et al. 2012, Kukulski et al. 2011 and Merrifield et al. 2004).

Different NPFs (Nucleating Promoting Factors), proteins that activate Arp2/3, are essential for endocytic budding: (1) Las17/WASP, (2) myosin I (Myo3 or Myo5) in a complex with Vrp1/WIP, (3) Pan1/Intersectin, and (4) Abp1 (Evangelista et al. 2000, Geli et al. 2000, Goode et al. 2001, Lechler et al. 2000, Lechler et al. 2001, Sun et al. 2006 and Winter et al. 1999). Las17/WASP and myosin I (with Vrp1) are categorized as class I NPFs because they bind actin monomers and have strong NPF activity (Sun et al. 2006).

1.3. Type I myosins

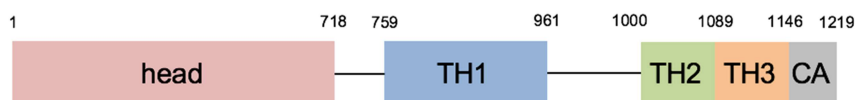


Figure 2: Myo5p domains. Head is the motor domain. TH(1-3) are tail homology domains. CA stands for Central and Acidic domain.

Type I myosins are considered unconventional within the myosin superfamily because they are single headed and non-processive (Pollard et al. 1991). They are ubiquitous, ancient proteins with a central role in eukaryotic cell biology. Myosin I proteins constitute a large family of ubiquitous actin/ATP-dependent molecular motors with a 110-130 kDa heavy chain and 1-6 light chains (Hasson & Mooseker 1995) that can be divided into two subclasses based on sequence homology of their motor domains (Hasson & Mooseker 1995). These proteins, as other types of myosins, bear a head or motor domain and a tail domain separated by a neck domain (Figure 2). The tail domain of myosins-I consists of three distinct functional subdomains, termed tail homology (TH)I-3 (Figure 2). TH-1 is rich in basic amino acids and is involved in membrane/acidic phospholipid binding (Pollard et al. 1991). The TH-2 domain is an alanine- and proline-rich region that contains an ATP-independent actin-binding site and the TH-3 domain includes a Src homology region 3 (SH3) domain, a type of domain present in a variety of proteins associated with the organization of the actin cytoskeleton and with signal transduction. The SH3 domain mediates protein-protein interactions through binding to proline-rich regions. Fungal myosins I also bear a Central and Acidic (CA) domain functionally homologous to those present in NPFs such as WASP or WAVE. The central and acidic domains are essential for binding and activation of the actin nucleating activity of the Arp2/3 complex.

Between the motor and tail domains, there is a neck domain which consists of one or two IQ consensus motif (IQXXRXXXXR), which constitute binding sites for small EF-hand-containing proteins like calmodulin (Grötsch et al. 2010 and Geli et al. 1998), which work as myosin light-chains and are thought to confer Ca^{2+} sensitivity to myosin regulation (Pollard et al. 1991).

Two functionally redundant genes encode for type I myosins in yeast: *MYO3* and *MYO5* (Geli & Riezman 1996 and Goodson et al. 1996). Both proteins localize at the plasma membrane and participate in the formation of endocytic vesicles. However, Myo5 seems to play a major role in endocytosis, since deletion of *MYO5* (but not *MYO3*) causes a strong defect in α -factor internalization at elevated temperatures (Geli & Riezman 1996). Deletion of *MYO5*, similar to deletion of *MYO3* (Goodson et al. 1996), does not lead to any observable alterations in growth. However, combination of both deletions in the same haploid results in a severe growth defects or even lethality depending on the strain background (Geli & Riezman 1996).

The Myo5 function as a NPFs is dependent on its SH3 domain which mediates binding to Vrp1. Vrp1 participates in the recruitment of Myo5 and is indispensable to trigger Myo5-induced actin polymerization (Anderson et al. 1998). Grötsch et al at 2010 found that Cmd1 dissociation from the myosin elongated its lifespan at cortical endocytic sites and triggered Myo5-induced actin polymerization *in vivo* and *in vitro* by releasing an autoinhibitory interaction and thereby, promoting binding to Vrp1. Fernández-Golbano et al. at 2014 subsequently found that the calmodulin dissociation is triggered by PI(4,5)P₂ and that Myo5-induced actin polymerization is coordinately terminated by the activity of the PI(4,5)P₂ phosphatase synaptojanin and the protein kinase Casein Kinase 2 (CK2). In addition, Myo5, as a member of the myosin superfamily, functions as a motor protein. Both biochemical activities (the mechanochemical activity and the actin polymerization promoting activity) act together to promote endocytic membrane invagination and vesicle budding (Anderson et al. 1998, Geli et al. 2000, Grosshans et al. 2006 and Sun et al. 2006).

1.4. Oxysterol Binding Proteins

The oxysterol-binding proteins (OSBP) belong to a large family of LTPs (Lipid Transfer Proteins) conserved from yeast to humans. They have been implicated in many cellular processes including signalling, vesicular trafficking, lipid metabolism, and non-vesicular sterol transfer (Raychaudhuri & Prinz 2010).

S. cerevisiae has 7 OSBPs related proteins (ORP) genes called *OSH1-7* that share a OSBP-related sterol-binding domain (ORD). Osh1, Osh2 and Osh3, through their FFAT domains, can bind to endoplasmic reticulum-resident proteins called vesicle-associated membrane protein-associated proteins (VAPs) in humans and Scs2 and Scs22 in yeast (Wyles et al. 2002; Loewen et al. 2003; Stefan et al. 2011).

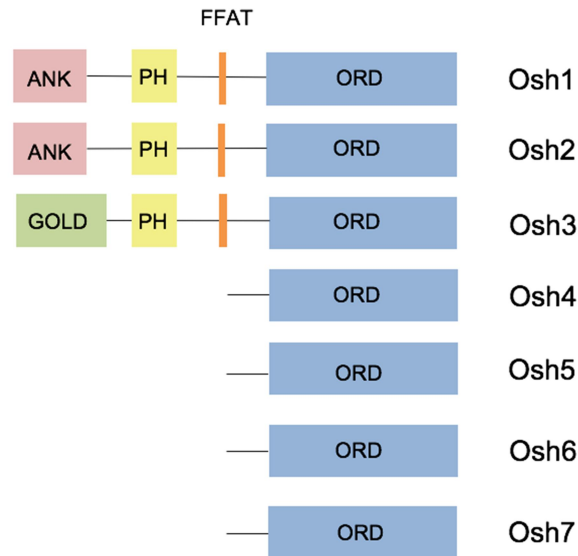


Figure 3: Osh proteins domains. ANK, ankyrin repeats; GOLD, Golgi localization domain; PH, pleckstrin homology domain; FFAT, di-phenylalanines within an acidic track; ORD, OSBP-related sterol-binding domain.

Some Osh proteins (Figure 3) also contain ankyrin repeats, PH domains and Golgi dynamics (GOLD) domains, which mediate protein-protein and protein-lipid interactions.

Osh2 and Osh3 localize to plasma membrane / endoplasmic reticulum (PM/ER) contact sites and serve to regulate the PM PI4P metabolism by activating the Sac1 PIP phosphatase (Stefan et al. 2011). Osh4/Kes1 also regulates PI4P levels at the Golgi (Li et al. 2002). In contrast, Osh1 localizes to the Golgi and the nuclear-vacuolar membrane junction sites (Levine & Munro 2001).

Osh proteins have a single over-lapping essential function since deletion of all seven ORPs in yeast is lethal. Compromising the function all seven Osh proteins results in a drastic change in cellular sterol composition (ergosterol levels increase by 3.5-fold) and defects in endocytosis (Beh et al. 2001).

1.5. Endoplasmic reticulum / plasma membrane contact sites

In the scientific community, increasing and recent interest has been put on the information transfer between intracellular organelles and the PM. The endoplasmic reticulum (ER) is the origin of the secretory pathway and it has essential roles in protein modification and quality control, lipid biosynthesis and calcium and cell signalling. This organelle in yeast consists of the nuclear envelope and a network lying just beneath the plasma membrane called the cortical ER (cER), with a few cytoplasmic ER tubules linking these two domains. The cortical ER forms a dynamic meshwork in the close vicinity underneath the PM; sheets and tubules of the ER are continuously rearranged (Prinz et al. 2000) and shaped by two protein families, the reticulons (Rtns) and DP1/Top1 (De Craene et al. 2006 and West et al. 2011).

In yeast, three conserved protein families serve as ER–PM tethers (Loewen et al. 2007 and Manford et al. 2012): the yeast VAP proteins Scs2/22, Ist2 and the tricalbin proteins Tcb1/2/3. The ER–PM tethering proteins are anchored in the ER and interact with the PM via cytoplasmic lipid-binding and protein-binding domains (Figure 4) (Manford et al. 2012).

The portion of the cER which has multiple focal attachments to the PM is specialized for synthesizing PM lipids and proteins.

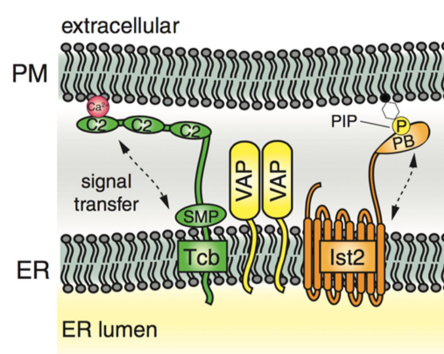


Figure 4: ER-PM tethering proteins.

All of the ER–PM tether proteins are integral ER membrane proteins that contain conserved cytoplasmic lipid-binding and protein-binding domains. The tricalbin (Tcb) proteins possess C2 domains that display Ca^{2+} -stimulated lipid binding activity and a conserved SMP domain that is sufficient for lipid binding and ER targeting. The Ist2 protein contains a carboxyl terminal polybasic domain (PB) proposed to bind PIP lipids at the PM. The lipid binding activities in the tether proteins may facilitate the transmission of signals between the PM and ER. The VAP proteins (Scs2 and Scs22 in yeast) recruit lipid-binding ORP family members to ER–PM contact sites; additional interactions with PM proteins and lipids may be involved in VAP tethering function (Stefan et al. 2013).

As mentioned above, ER also participates in the regulation of cell signalling networks. In particular, the PIP isoform PI4P serves as an essential signalling molecule in the control of cell growth and polarity, hormone and calcium signalling, and regulated secretion and endocytosis (Hammond et al. 2012). Notably, an ER-localized PIP phosphatase, named Sac1, regulates PI4P levels at ER–PM contact sites (Stefan et al. 2011). This process is mediated by the ER-localized Scs2 and Scs22 proteins and by Osh2 and Osh3 localized to ER–PM junctions (Figure 5).

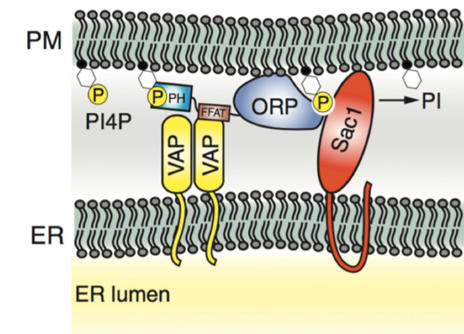


Figure 5: Phosphoinositide signalling. ER–PM contacts are also sites for regulation of PI4P levels in the PM (Manford et al. 2012 and Stefan et al. 2011). The ER-localized PIP phosphatase Sac1 is activated by ORPs family members at ER–PM contacts, resulting in PI4P turnover at the PM. This process is facilitated by VAPs in the ER (Stefan et al. 2012).

2. Preliminary results and Objectives

Unpublished Time-Resolved Electron Microscopy studies (Idrissi & Geli 2014) performed in the laboratory indicate that the endocytic invaginations become increasingly associated with the cortical ER as they mature (Figure 6). The results indicate that the association possibly occurs at the time when massive actin polymerization is initiated at endocytic sites and that it involves one or more endocytic proteins present at the junction between the plasma membrane and the endocytic invagination. Interestingly, Myo5, which is one of the proteins that initiates actin polymerization during the plasma membrane invagination, sits at this position (Idrissi et al. 2008) and it has been shown in genome wide screenings to interact with Osh2 (Gavin et al. 2006 and Tonikian et al. 2009), a protein that can generate ER/ PM contact sites. Based on these observations, we hypothesized that the Myo5/Osh2 interaction might participate in the formation of the ER/endocytic invagination contact sites and that this contact sites are required to initiate or complete endocytic budding.

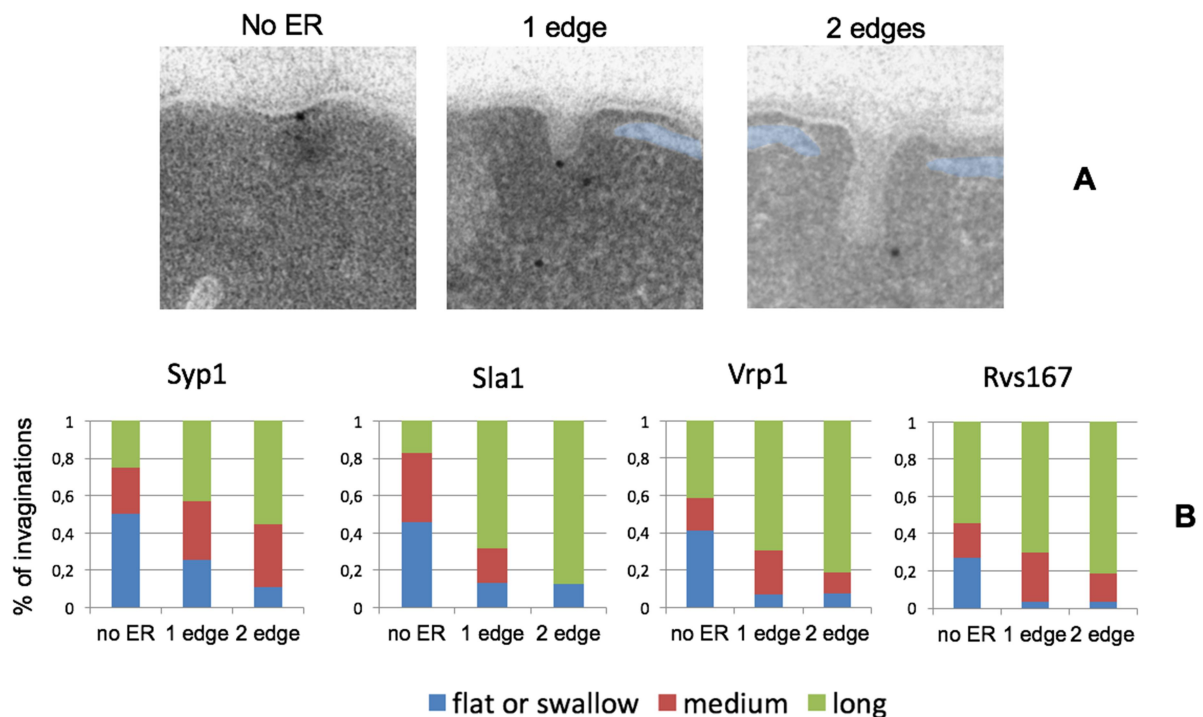


Figure 6: Association of the cortical ER and the endocytic invaginations. A. Electron micrographs of endocytic invaginations immunolabeled with gold particles against the endocytic coat components (Syp1: early coat protein, Sla1: late coat protein, Vrp1: binds to Myo5 constituting and NPF, and Rvs167: yeast amphysin) showing increasing association with the cortical endoplasmic reticulum (coloured in blue) as they elongate and mature. B. Graphs showing the percentage of swallow (< 50 nm in length), medium (50 to 100 nm in length) and long invaginations (>100 nm in length) associated to the cortical ER in non, one or both sites.

In this context, the specific objectives of this project were:

- To confirm the interaction between Myo5 and Osh2 by Two Hybrid assays and immunoprecipitation experiments.
- To investigate if other ORPs interact with Myo5.
- To define the Myo5 and ORPs domains involved in the putative interactions.
- To design mutations in Myo5 and in the ORPs that specifically disrupt the interactions. These mutations would constitute a necessary tool to analyse the role of the putative ER/PM contact sites in the budding process itself.

3. Materials and methods

3.1. Plasmids

All plasmids used in this project are described in tables 6 and 7.

3.2. Polymerase Chain Reaction

PCRs (Polymerase Chain Reactions) are used to obtain a high number of copies of a specific DNA fragment using a very limited quantity of the original DNA which acts as a template. A DNA polymerase with proof reading activity, in our case, Vent polymerase (New England Biolabs, Inc), catalyses the reaction in the presence of two oligonucleotides (DNA sequences which are complementary to a specific region of the DNA template), one forward and the other reverse, which act as primers.

PCRs amplification conditions are shown in table 1. PCRs components and reagents are shown in table 2. PCRs were performed using a TRIO thermoblock (Biometra GmbH).

Initialization	95° C	5 min
Denaturation	95° C	1 min
Annealing	50° C	1 min
Elongation	72 °C	40 sec / kb
Final elongation	72° C	10 min
Final hold	4° C	∞

Table 1: PCRs amplification conditions.

Template DNA	1 µl
Forward oligonucleotide	0,5 µl
Reverse oligonucleotide	0,5 µl
MgSO₄	1 µl
dNTPs mix 2mM	10 µl
VENT polymerase	1 µl
Polymerase buffer	10 µl
DMSO	4 µl
MiliQ H₂O	72 µl

Table 2: PCRs components and their quantities for a 100 µl PCR.

A series of PCRs was performed with the oligonucleotides indicated in table 3 and pFA6A-3HA-HiS3MX6 (Figure 7) (Longtine et al. 1998) as template to generate cassettes encoding the triple HA epitope and the *HIS3* marker flanked by 40 oligonucleotides immediately upstream and immediately downstream of the stop codon of the *OSH1*, *OSH2*, *OSH3*, *OSH4*, *OSH5*, *OSH6*, *OSH7* genes. It was clear that the 7 PCRs were satisfactory because, the size of DNA fragment fit the predicted 1742 bp of the cassette. These cassettes were purified using NucleoSpin® Gel and PCR Clean-up kit and protocol.

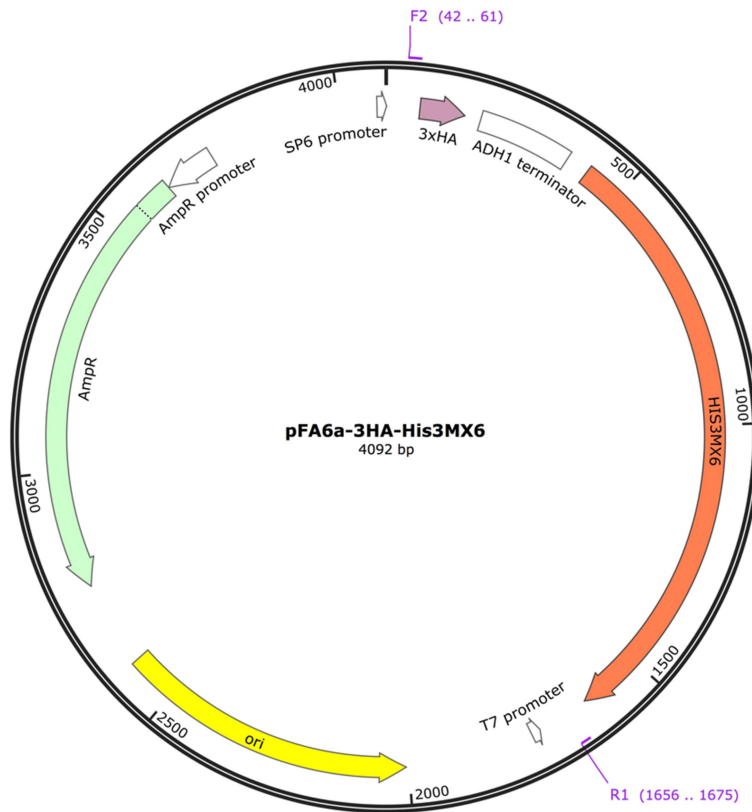


Figure 7: pFA6a-3HA-His3MX6. This is the plasmid used to tag all of the Osh proteins. To amplify the cassette, F2 and R1 derived oligonucleotides were used, therefore amplifying 3xHA-His3MX6. (Longtine et al. 1998)

F2	R1	Protein tagged
AAGAAAAATCATGACTTTAAAGATTGTG CTGATATTTTCCGGATCCCCGGGTTAATT AA	ATACAAATGAACGAGTGTTATTGTGACT ACATTGCACAGCGAATTCGAGCTCGTTT AAAC	Osh1
AAGAAGAGATCATGATTTGAAAGATTGTG GTGACATTTTCCGGATCCCCGGGTTAATT AA	ATACAAGTACCAGGAAAAAAGCTCGCA TAAAAAAGCGTGGAATTCGAGCTCGT TTAAAC	Osh2
AAGAAAGAAGCATGATTGGTCTGATATTT CTCAACTCTGGCGGATCCCCGGGTTAAT TAA	CAAAGGGGGGAAAAAAGTTCACCTTGAT GTCATCAAGGCATGAATTCGAGCTCGT TTAAAC	Osh3
CAAAGAGAGTTGTGGGACGAAGAAAAGG AAATTGTTTTGCGGATCCCCGGGTTAATT AA	ATTAGTGCAACGGTAACAAGTTGTTACT TTATCGTTCTCCGAATTCGAGCTCGTTT AAAC	Osh4
GATAAAAATTTGTGGATGAGGGAGAACG AAATTACTATACGGATCCCCGGGTTAATT AA	GTATTAATTTTTGATATTTATTCTTTAAA AACATTTATAGAATTCGAGCTCGTTTAA AC	Osh5
GAAGATGATTGAAAACGAAAAGCAGAAC CCAGCAAAACAACGGATCCCCGGGTTAA TTAA	AATCTATAATTTACAACAAATATCATATC CAACATATACAGAATTCGAGCTCGTTTA AAC	Osh6
TCTATTCCGGCTTATAAAAAGCATGGAAT CCAAAAGAATCGGATCCCCGGGTTAATT AA	TGAGAAATCGTACTAGTATAATTTAAAAT AGAATGAGAAGCGAATTCGAGCTCGTT TAAAC	Osh7

Table 3: Oligonucleotides used to tag Osh1-7 genes.

3.3. Yeast culture, transformation and strains

Saccharomyces cerevisiae culture was carried out following the standard protocols (Sambrook and Russell, 2012). All liquid cultures were grown at 28°C with constant shaking. Optic density of each culture was measured spectrophotometrically to define the growth stage.

Transformation of yeast was accomplished by the lithium acetate method (Ito et al. 1983): First, a 10 ml liquid culture of the yeast strain to transform was grown at OD 0,4-0,8. Then, cells were harvested (3200 rpm 5') in a 15 ml falcon tube, washed with 1,5 ml of Li-TE and harvested again. Afterwards, the pellet was resuspended in 50 µl of Li-TE 2x and set aside at RT while preparing the DNA. For each transformation, a 1,5 ml Eppendorf with 3 µl of carrier DNA Herring Sperm, 2 µg of the plasmid DNA or PCR product of interest, 50 µl of cells and 150 µl of PEG 50% were mixed. The cells were then incubated at RT for 25 minutes and heat shocked at 42°C for 15 minutes to facilitate the entrance of the DNA into the cells. Finally, 200 µl of TE (10 mM Tris HCl and 1 mM EDTA pH 7.5) were added to each eppendorf and cells were plated on the appropriate minimal media agar plates. Colonies were grown for 3 days at 28° C.

In detail, SCMIG136, which lacks the gene encoding Myo5 and bears a mutation in the *HIS3* gene, which causes an auxotrophy for Histidine (*Matalpha his3 leu2 lys2 ura3 myo5D::KMX (yhr109w::KMX)*), was transformed using the LiAc method with the suitable DNA cassette. As designed, upon homologous recombination in the proper locus (figure 8), *OSH1-7* genes would be genome edited to express at their C-terminus 3 copies of Haemagglutinin (HA) epitope YPYDVPDYA. The transformed strains were plated in SDC-HIS media to select the colonies which did integrate the cassette. Once the colonies which had integrated the *HIS3MX* cassette were selected and replated, we proceed to check by immunoblot if the protein of interest was indeed genome edited to express the HA epitope.

Strains SCMIG1208, SCMIG1209, SCMIG1210 were generated by the p33protA-MYO5 episomal plasmid introduction. Strains 1-64 were generated by the suitable episomal plasmid introduction (Table 8). Strains bearing episomal plasmids were grown on SDC (synthetic dextrose complete: 2% de glucose (Duchefa), 0.67% yeast nitrogen basis (Difco) and 0.075% de CSM (*Complete Synthetic Mix*, Qbiogene)) lacking the appropriate nutrient (Dulic et al., 1991) at 28°C.

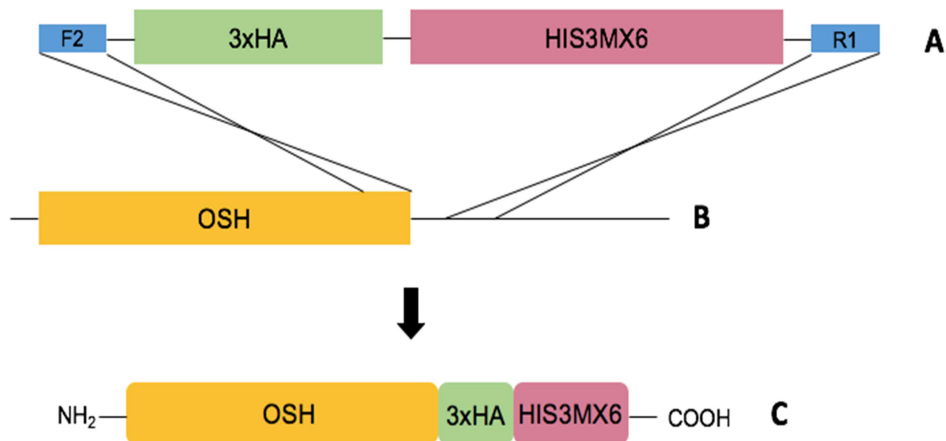


Figure 8: Diagram representing the event of homologous recombination between PCR product and the C-terminus of an *OSH* gene. A, PCR product flanked by F2 and R1 primers; B: yeast genome focused on *OSH* proteins; C: fusion protein result of homologous recombination between A and B.

3.4. Protein extractions

Total yeast protein extractions were performed as described (Horvath & Riezman 1994). First, a 5 ml liquid culture of yeast was grown at RT in a 50 ml falcon overnight. The day after, the culture was diluted to 20 ml so that OD was 0,15. When the culture was at OD = 0'4 – 0'6, cells were harvested (3200 rpm 5 minutes) in a falcon at 4°C. Its supernatant was discarded and the cells were transferred to a 1,5 ml eppendorf using 1 ml of pre-chilled PBS (40 mg NaCl, 1 mg KCl, 9,02 mg Na₂HPO₄ 2x H₂O and 1,2 mg KH₂PO₄). After that, cells were harvested again and their supernatant was discarded. Then, cells were frozen in liquid nitrogen and stored at -80°C until its use.

At the day of the protein extraction, 50 µl of prechilled PBS containing protease inhibitors (PMSF (2 mM in DMSO), leupeptine (10 µg/ml in water), antipain (50 µg/ml in water), pepstatin (2 µg/ ml in ethanol) and aprotinin (2 µg/ml in water) and 150 µl of acid-washed glass beads were added to each sample. Then, samples were vortexed during 20 minutes at 4°C. After that, each sample was spun at 700 g during 15 minutes and the supernatant, where the proteins remain, was recovered. Then, protein concentration of each sample was measured with the BioRad Kit (Bio-Rad Laboratories). Finally, extracts were diluted to 10 µg/µl with PBS and the same volume of SDS-PAGE sample buffer (4% SDS, 20% glycerol, 200 mM DTT and 126 mM Tris-HCl pH 6,8) was added. The mixture was boiled for 5 minutes. For the immunoblot, 5 to 40 µg of total protein were loaded.

3.5. Sodium Dodecyl Sulfate - Polyacrylamide Gel Electrophoresis

Sodium Dodecyl Sulfate - Polyacrylamide Gel Electrophoresis (SDS-PAGE) is a technique in which proteins denatured and coupled to the ionic detergent SDS are separated according to mass as they are forced through a sieving gel matrix by an electrical current (100 V) during 90 minutes. SDS-PAGE was performed as described (Laemmli, 1970) using a minigel system (Bio-Rad Laboratories). 10% acrylamide gels were used (see annex section 4 for composition). PageRuler™ Plus Prestained Protein Ladder from Thermo Fisher Scientific was used as a kDa marker.

3.6. Immunoblot

Immunoblots were performed as described (Geli et al. 1998). Briefly, after SDS-PAGE, proteins were transferred from the polyacrylamide gel to a nitrocellulose membrane (Potran BA85 Cellulose nitrate Schleicher and Schuell 401199) using a transfer buffer (390 mM Glycine, 480 mM Tris-Base, 0.37 % SDS, pH=8,3) during 90 minutes at 100 V using Biorad Mini-Trans blot. Afterwards, Ponceau staining (0.3 % Ponceau Red and 3 % TCA) was applied to the membrane to check whether proteins were transferred correctly. Next, the membrane was incubated with 5 ml of blocking buffer (PBS, 1% NP40 (V/V) + 2% lyophilized milk (W/V)) during 30 minutes.

The membrane was then incubated with either a peroxidase-conjugated rat monoclonal anti-HA-peroxidase (Roche) antibody to detect the HA epitope or Rabbit PAP (peroxidase anti-peroxidase complex) (Sigma) to detect ProtA-tagged proteins. After the incubation, membranes were washed 3 times with blocking buffer and 3 times with PBS. An enhanced chemiluminescence detection kit (Amersham ECL Western Blotting Detection Reagent) was used for detection of peroxidase-conjugated antibodies. Finally, membranes were exposed to KODAK-XAR X-ray films during different times (from 1 minute to 1 hour).

Protein extracts from SCMIG136 were used as negative controls. Protein extracts from colonies showing specific bands with the expected size (Table 4) were considered positive. Homologous recombination efficiency between 3HA-HIS3MX cassette and the C-terminus of *OSH1-7* genes is shown in table 5. An immunoblot decorated

PROTEIN	MOLECULAR WEIGHT (kDa)
Osh1	135,0558
Osh2	145,7865
Osh3	113,7690
Osh4	49,4833
Osh5	49,5034
Osh6	51,5925
Osh7	49,8031

Table 4: OSH proteins and their predicted molecular weights. 3HA epitope molecular weight is 4,37 kDa.

with antiHA of the epitope tagged yeast strains finally selected is presented in figure

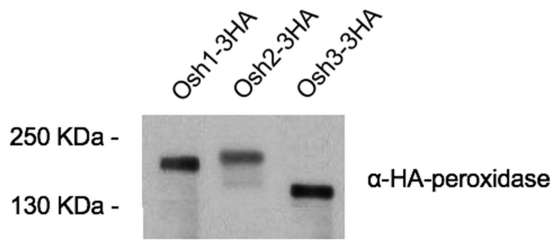


Figure 9: Anti-HA immunoblot from yeast extracts expressing OSH1-3HA, OSH2-3HA or OSH3-3HA.

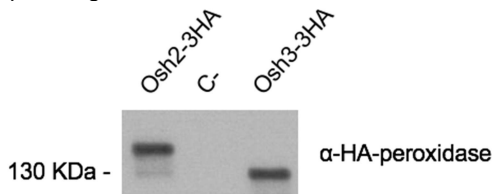
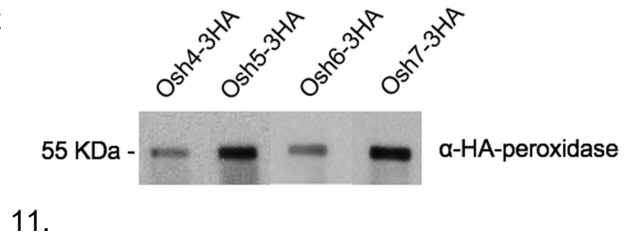


Figure 11: Anti-HA immunoblot from yeast extracts expressing either OSH2-3HA or OSH3-3HA. As a negative control, a yeast extract from SCMIG136 was used.



11.

GENE	HOMOLOGOUS RECOMBINATION EFFICIENCY
<i>OSH1</i>	1/12
<i>OSH2</i>	1/4
<i>OSH3</i>	1/4
<i>OSH4</i>	2/4
<i>OSH5</i>	1/4
<i>OSH6</i>	1/4
<i>OSH7</i>	1/4

Figure 10: Anti-HA immunoblot from yeast extracts expressing OSH4-3HA, OSH5-3HA, OSH6-3HA, or OSH7-3HA.

Table 5: Homologous recombination efficiency between 3HA-HIS3MX cassette and the C-terminus of *OSH1-7* genes.

3.7. Immunoprecipitation (IP) and co-immunoprecipitation (co-IP)

Immunoprecipitation is a method that enables the purification of a protein from a total protein cell extract. A cell extract is incubated with agarose or sepharose beads conjugated to an antibody that recognises the protein. Beads are pulled down by gravity or centrifugation at low speed and after several rounds of washes, the protein of interest is segregated from the rest. The protein can be eluted by denaturing the sample on SDS-PAGE sample buffer at 90°C and can then be separated by SDS-PAGE for immunoblot analysis.

If the initial protein extract is prepared under non denaturing conditions, proteins that stably interact with the immunoprecipitated protein will co-immunoprecipitate. The Co-IP is a classic technology widely used to test protein-protein interactions. When the bait protein is already eluted, we can check by immunoblot analysis if there is a protein (prey protein) forming

complex with the bait protein by incubating the membrane with an antibody that binds to prey protein.

Both techniques require to work at 4° C during the whole experiment because they deal with proteins very prone to degradation.

First, 300 ml cultures at OD = 0,4 – 0,6 of the following strains were obtained:

- SCMIG1208 (Myo5-2ProtA)
- SCMIG1202 (Osh2-3HA) / SCMIG1203 (Osh3-3HA)
- SCMIG1209 (Osh2-3HA + Myo5-2ProtA) / SCMIG1210 (Osh3-3HA + Myo5-2ProtA)

Then, yeast cultures were chilled for 10-15 minutes and harvested (3200 rpm 5 minutes).

After that, cells were washed with 1-2 ml of IP buffer (50 mM Tris HCl pH 7.5, 5 mM EDTA, 150 mM NaCl), the mix was transferred to 2 ml eppendorfs and cells were harvested again. Pellets obtained were stored at -80°C until use.

Once pellets were obtained, 150 µl of IP buffer with proteases inhibitors (PMSF (2 mM in DMSO), leupeptine (10 µg/ml in water), antipain (50 µg/ml in water), pepstatin (2 µg/ml in ethanol) and aprotinin (2 µg/ml in water) and 300 µl of glass beads were added to each of them. Then cells were lysated by vortexing during 20 minutes with 30 seconds intervals on ice.

To separate the protein extract from the unbroken cells and the cell debris, cell lysates were spun at 700g for 15 minutes at 4°C and the supernatants were recovered into a 1,5 ml eppendorf. Then, samples were centrifuged at 13000 rpm during 20' and pellets were resuspended in IPT (IP buffer 1%Triton-X100) buffer with inhibitors. Protein concentration was measured using the BioRad kit and 100 µg of each sample were kept to load as the input. For each culture, IPT with protease inhibitors was added so as to have a total volume of 1 ml with the same amount of total protein per sample. The tubes were incubated on ice for 30 minutes and spun at 700 g 15' at 4°C.

The supernatants were then transferred to siliconized tubs and 30 µl of IgG sepharose beads (50%) or anti-HA-agarose beads (50%) were added to each tube. Samples were then incubated in a roller for 1 hour at 4°C.

Afterwards, beads were pelleted at 500g for 30 seconds at 4°C and the supernatant was discarded. Then beads of each tube were washed 3 times with 1 ml of IPT buffer and 3 times with 1 ml of IP buffer. Finally, bead pellets were drained with a Hamilton and 40 µl of SDS-

PAGE SB without DTT was added to each pellet. Tubes were boiled for 5 minutes and shortly spun.

The supernatants were recovered and 4 μ l of DTT were added to each sample, and 10 μ l were loaded for immunoblot analysis of the immunoprecipitated and co-immunoprecipitated proteins.

3.8. Two Hybrid

Two Hybrid assay enables the detection of protein-protein interactions *in vivo*. For the detection of a protein-protein interaction the target protein called the bait is fused to a DNA binding domain such as LexA and the putative interacting protein called the prey is fused to a transcriptional activation domain such as B42 (Gyuris et al. 1993). Both plasmids are then introduced through LiAc transformation in a yeast strain bearing a reporter gene such as β -galactosidase enzyme bearing LexA binding motif in its promoter. When the proteins of interest interact, a LexA-B42 transcription factor is reconstituted, which will promote transcription of the reporter. This enzyme generates a blue precipitate in the presence of X-GAL. Therefore, when there is interaction between the bait and the prey proteins, a blue precipitate appears, and when not, the cells are uncoloured (Figure 12).

The Two Hybrid system used was the one described at Gyuris et al. 1993. Plasmids pEG202, pJG4-5, pSH18-34 and the strain EGY48 were kindly provided by R.Brent (MGM, Boston). To measure β -galactosidase activity, EGY48 cells bearing the *lexAop-lacZ* reporter plasmid pSH18-34 were co-transformed with the appropriate pEG202 and pJG4-5 derived plasmids (Table 6) and selected in SDC-URA-HIS-TRP. For the induction of proteins under a GAL1-promoter, yeast cells were inoculated on X-Gal (5-bromo-4-chloro-3-indolyl- β -D-galactopyranoside)-containing SD/Gal/Raf-His-Trp-Ura plates [0.67% yeast nitrogen base (Difco), 7 g/l Na_2HPO_4 , 3 g/l NaH_2PO_4 , 2% galactose, 1% raffinose, 40

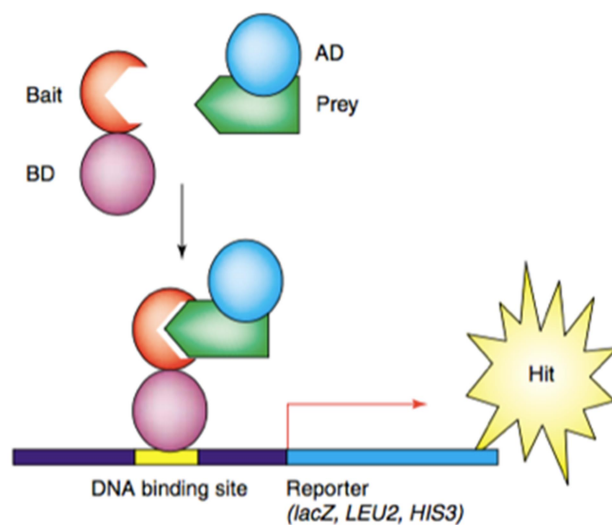


Figure 12: The basic yeast two-hybrid system. Bait proteins fused to a DNA binding domain (BD) are tested for the interaction with a prey protein fused to a transcriptional activation domain (AD). Bait and prey fusions are co-transformed into the same yeast cells. Interaction of the bait and the prey reconstitutes transcription factor activity, which then activates expression of the reporter gene such as *lacZ*, which enables a colorimetric readout (Hollingsworth & White 2004).

mg/ml leucine, 80 mg/l X-Gal (Sigma Chemicals Co.), 2% agar pH 7]. Pictures were taken after a 36h incubation at 24°C.

4. RESULTS

4.1. Myo5 interacts with Osh2 and Osh3 in a Two Hybrid assay

Genome wide screenings indicated that Myo5 might interact with Osh2 (Gavin et al. 2006 and Tonikian et al. 2009). To confirm this result and to investigate if other yeast ORPs might interact with Myo5, we conducted several Two Hybrid assays using the Myo5 Tail fused to the LexA binding motif and the complete ORFs of the ORPs Osh4, Osh5, Osh6 and Osh7 fused to B42 and N and C-terminal fragments of the longer proteins Osh1, Osh2 and Osh3 also bound to B42 (Figure 13). With this purpose, the EGY48 strain bearing an episomal *URA3* plasmid with the beta-lactamase reporter gene under the control of a promoter bearing LexA binding sites, was co-transformed with either the plasmid encoding the LexA-Myo5 fusion protein or an unrelated protein (LexA-bicoid) as a negative control, with the different ORP constructs fused to B42, indicated in figure 13, the B42 alone as a negative control, and B42 fused to Vrp1 as a positive control (Geli et al. 2000). The transformed strains were selected in SDC –URA –HIS –TRP. For the Two Hybrid assay, a patch of cells was replicated on media lacking glucose and bearing raffinose and galactose for the induction of the LexA and B42 fusion proteins, also bearing X-Gal for the detection of the beta-lactamase activity. Photos of the plates were taken after 36h incubation at 25°C.

As previously described (Geli et al. 2000), we could detect a specific interaction of the Myo5 tail with Vrp1. In addition, we confirmed the interaction of Osh2 with Myo5 and we mapped it to the N-terminus of Osh2, a fragment lacking the OSBP-related sterol-binding domain (ORD) and bearing the PH domain, the FFAT motif and the Ankyrin repeats. Interestingly, the very same fragment of Osh1, sharing 66.3% of similarity with Osh2, did not show any interaction with Myo5. The C-terminal fragment of Osh2 bearing the ORD did not show any interaction with Myo5 neither. Consistent with this observation, neither of the ORPs mainly composed by the ORD (Osh4 to Osh7) showed a specific interaction with Myo5. Interestingly though, we could demonstrate a weak but specific interaction between Osh3 and Myo5, which was not previously described. Similar to Osh2 the interaction between Myo5 and Osh3 required the N- terminus of the Osh3 protein lacking the ORD and bearing the PH domain, the FFAT motif and the GOLD domain.

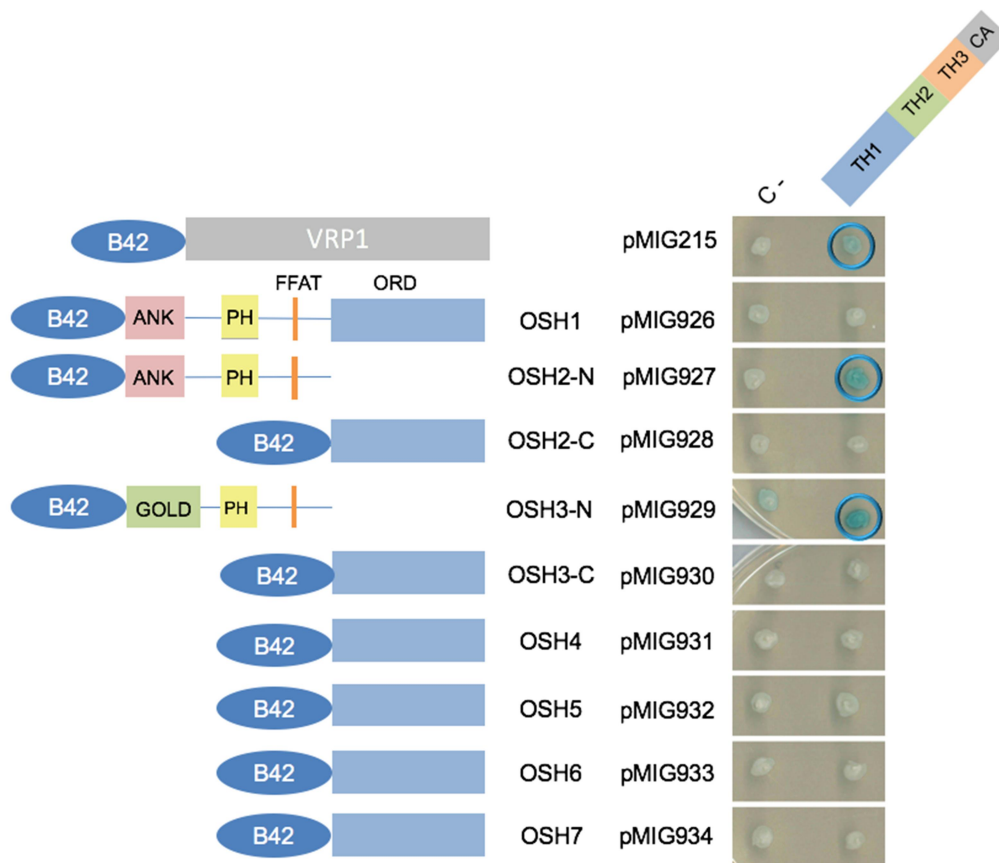


Figure 13: Two-hybrid assay 1. Two-hybrid assays in which the bait protein was Myo5 tail (pEG202MYO5), and the prey proteins were the Osh proteins. Negative controls: LexA-bicoid (pRFHM1) and B42 (pJG4-5; not shown). Positive control: B42-Vrp1 (pJG4-5END5).

4.2. Myo5 interacts with Osh2 and Osh3 using different domains

From that point, we tried to define the Myo5 domains required for its interaction with Osh2 and Osh3. For this purpose, plasmids bearing the Osh2 and Osh3 N-terminal fragment fused to B42, B42-Vrp1 as positive control, or the empty plasmid as negative control, were cotransformed in the Two Hybrid reporter strain, with plasmids encoding the LexA-Myo5 fragments indicated in figures 14 and 15, or the lexA-bicoid as a negative control. As previously reported (Anderson et al. 1998), the Myo5 region interacting with Vrp1 was specifically mapped to the SH3 domain. Interestingly, Osh2 also specifically interacted with the Myo5 SH3 domain (Figure 14), but the interaction with Osh3 mapped to the TH1 and TH2 domains, Myo5 domains that were thought to exclusively mediate the interaction of Myo5 with lipids and actin, respectively (Figure 15).

4.3. The interaction of Myo5 and Osh2 probably involves a polyproline motif in Osh2.

The SH3 domains are known to mediate the interaction with polyproline rich sequences. The structure of a number of SH3 domains in complex with their ligands has been solved and has demonstrated the essential role of a conserved tryptophan in the SH3 domain which lies in the position W1123 of Myo5. Consistent with this observation, mutation of the Myo5 W1123 to S completely disrupted the interaction of Myo5 with Vrp1, which is known to be mediated by polyP motifs of Vrp1 (Grötsch et al. 2010). To investigate if the Myo5-Osh2 interaction might involve a polyP motif in Osh2, the effect of the Myo5 W1123S mutation on the Myo5-Osh2 interaction was tested using the Two Hybrid assay. As shown in Figure 16, the W1123S mutation disrupted both, the Myo5 interaction with Vrp1 and with Osh2.

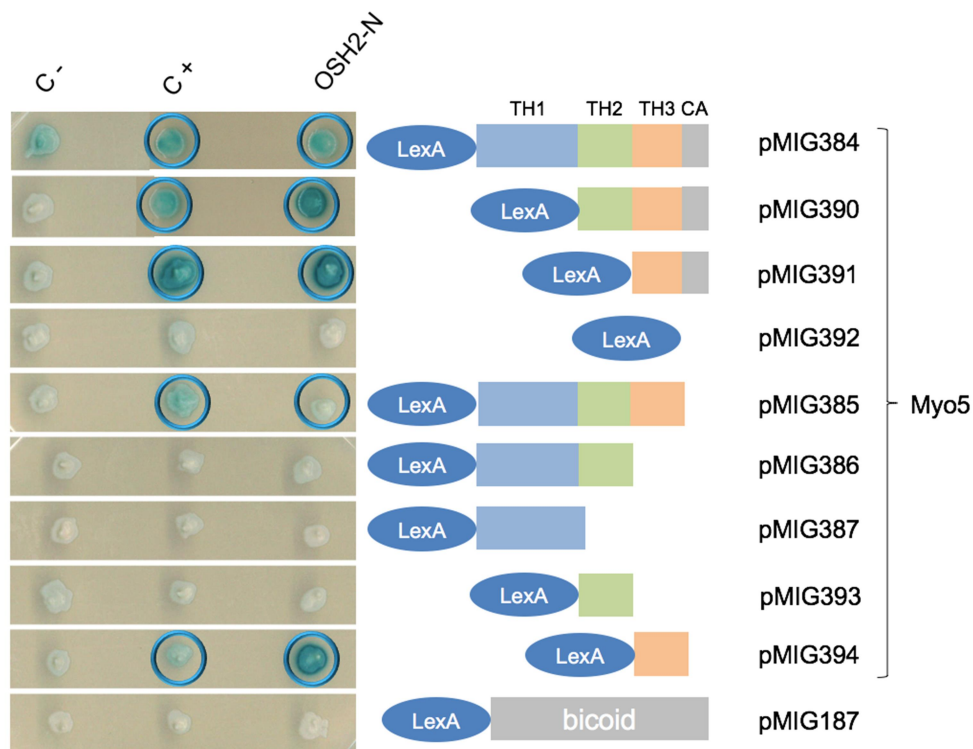


Figure 14: Two Hybrid assay 2. Two Hybrid assay in which the bait proteins were Myo5 constructions and the prey protein was OSH2-N (pJG4-5OSH2-N). Negative controls: LexA-bicoid (pRFHM1) and B42 (pJG4-5). Positive control: B42-Vrp1 (pJG4-5END5).

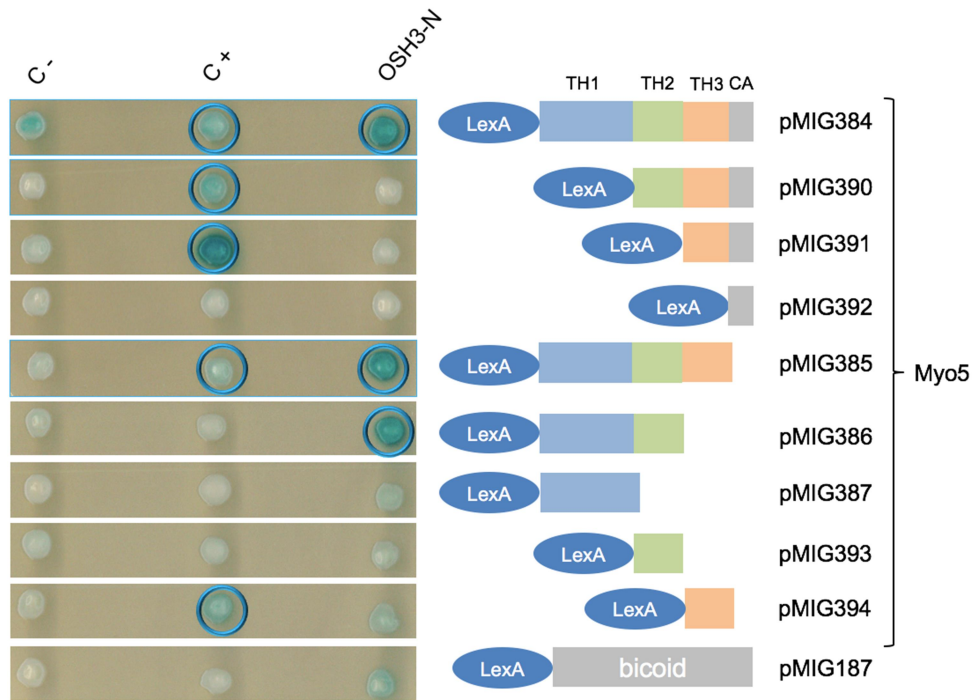


Figure 15: Two Hybrid assay 3. Two Hybrid assay in which the bait proteins were Myo5 and its variations and the prey protein was OSH3-N (pJG4-5OSH3-N). Negative controls: LexA-bicoid (pRFHM1) and B42 (pJG4-5). Positive control: B42-Vrp1 (pJG4-5END5).

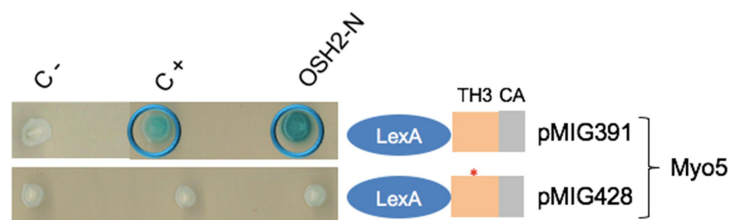


Figure 16: Two Hybrid assay 4. Two Hybrid assay in which the bait proteins were TH3-CA domains of Myo5 (pEG202(SH3, TH2c)) and the same construction but with the mutation W1123S in TH3 domain (pEG202(SH3*,TH2c)) and the prey protein was OSH2-N (pJG4- 5OSH2-N). Negative controls: LexA-bicoid (pRFHM1) and B42 (pJG4-5; not shown). Positive control: B42-Vrp1 (pJG4-5END5).

4.4. Analysis of the interaction between Myo5 and ORPs by co-immunoprecipitation

To obtain additional evidence demonstrating that Myo5 and some of the endogenous yeast ORPs interact, we decided to perform co-immunoprecipitation assays between the yeast ORPs Osh2 and Osh3 genome edited to express 3 copies of the HA epitope at their C-terminus, and a Myo5 version N-terminally tagged with 2 copies of Protein A, expressed from a low copy plasmid (p33ProtA-MYO5) as the only source of Myo5 (Gietz & Akio 1988).

For the IPs and the co-IPs, a 13000 g pellet (P13) from a total protein cell extract was used as a starting material because ORPs are not very abundant in yeast cells (Ghaemmaghani et al. 2003 and Kulak et al. 2014) and the P13 fraction is highly enrich in plasma membrane and endoplasmic reticulum markers as well as Myo5 and ORPs. As shown in figure 17 immunoprecipitation of 2ProtA-Myo5 with IgG-Sepharose did not bring down significant amounts of Osh3-HA but it specifically pulled down Osh2-HA from the P13 fraction (Figure 18). The signal detected by the HA antibody specifically recognized the Osh2-HA because it was absent from the immunoprecipitation when a strain untagged for *OSH2* was used. Further, Osh2-3HA specifically co-immunoprecipitated with 2ProtA-Myo5 on the IgG-Sepharose beads since the Osh2-HA signal was lost when a strain expressing Myo5 instead of ProtA-Myo5 was used in the assay. However, we could not co-immunoprecipitate Osh3-3HA with 2ProtA- Myo5.

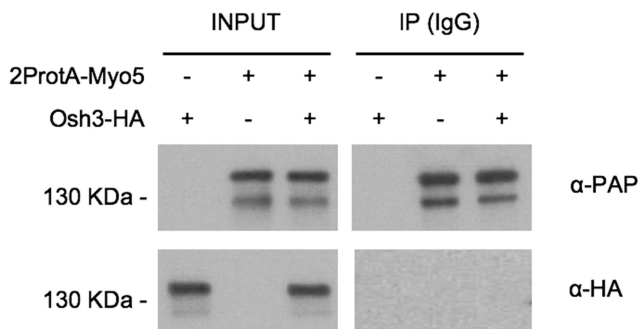
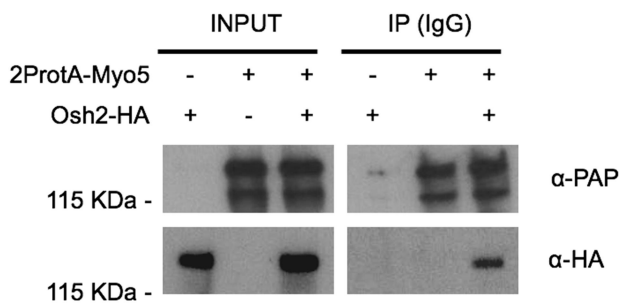


Figure 18: PAP and anti-HA immunoblots of IgG-Sepharose immunoprecipitations from cells expressing Osh2-HA and/or Myo5-ProtA. From J. Encinar

Figure
of IgG
from c
Myo5-P

5. DISCUSSION

5.1. **Myo5 interacts with Osh2 and probably Osh3**

The analysis of the Myo5 interaction with the yeast ORPs using Two-Hybrid assays (Figures 13-16) has provided compelling evidence indicating that the myosin-I specifically interacts with Osh2 and Osh3. Genome wide studies had already anticipated the Osh2/Myo5 interaction. In contrast though, the interaction between Osh3 and Myo5 was previously undescribed. The Myo5/Osh2 and /Osh3 interaction is consistent with the localization of these ORPs at the plasma membrane and with the hypothesis that they could mediate the formation of contact sites between the ER and the endocytic sites. The observation that Osh2 and Osh3 bind different Myo5 domains (see below) might suggest that simultaneous binding of Myo5 to both ORPs is needed to efficiently establish the ER / endocytic sites contact sites. Myo5 does not seem to interact with any of the other ORPs present at the cortical ER in contact with the plasma membrane (Osh6 and Osh7) (Schulz et al. 2009). This observation indicates that Osh2 and Osh3 might play a specific role in endocytic uptake, which is not shared by the other ORPs.

The intensity of the Two Hybrid signals indicates that the interaction between Myo5 and Osh2 is stronger than of the Myo5 Osh3 pair. This could be explained by artefactual differences in the expression of the constructs used in the Two Hybrid assays or in differences in their ability to enter the nucleus. However, consistent with the view that the Myo5/Osh2 interaction is stronger than the Myo5/Osh3 interaction, we could immunoprecipitate the endogenous Osh2 with the Myo5 but not Osh3. Alternatively, the interaction between Myo5 and Osh3 could occur in a compartment that it is not enriched in the P13 fraction. Consistent with this hypothesis, Osh3 has a GOLD domain that could potentially direct the protein to the Golgi apparatus.

Even though Osh1 shares 66% similarity with Osh2 at the amino acid level, the result that Myo5 does not interact with Osh1 is somehow consistent with the previous observation that this ORP localizes to vacuolar-ER contact sites (Levine & Munro 2001) and further indicates that, despite the sequence homology and the similarities between their domain organization, they are not merely functionally redundant homologs.

Osh2 and Osh3 interact with the ER integral membrane proteins Scs2 and Scs22 (Kaiser et al. 2005 and Loewen et al. 2003), the homologs of VAPs in mammals, and modulate the activity of the ER PI4P phosphatase Sac1 on the phosphoinositide pool of the plasma membrane (Stefan et al. 2011). We have recently demonstrated that hydrolysis of PI(4,5)P₂

at endocytic sites is required to initiate scission of the endocytic invaginations (Fernández-Golbano et al. 2014).

We could then hypothesize that the Myo5/ORPs interaction bridge the endocytic contact sites to the Scs2 and Scs22 proteins to bring Sac1 to initiate vesicle scission (Figure 19). Consistent with this, unpublished results from J. Encinar indicate that Osh2 and Sac1 mutants have defects in vesicles scission. Alternatively or in addition, the ER could constrict the endocytic invagination to physically promote fission as it has been proposed for endosome and mitochondria fission.

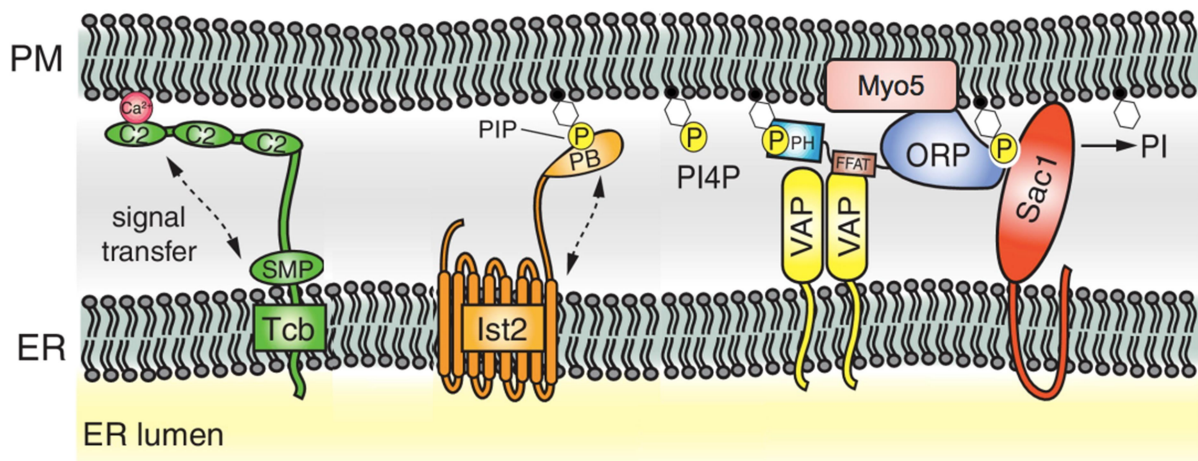


Figure 19: Molecular model for ER-PM contact sites in which Myo5-Osh2 interaction takes part. Tcb: Tricalbins, orthologues of the synaptotagmins. Ist2: Related to mammalian TMEM16 ion channels. VAP/Scs22/2: Vesicle-associated membrane protein-associated proteins. Osh2 (Oxysterol-binding homology proteins) consists of Ankyrin repeats (not shown here), PH domain, FFAT domain and ORP domain. Sac1: Phosphoinositide phosphatase. Modified from Stefan et al. 2013.

5.2. Osh2 and Osh3 interact with the SH3 and TH1/TH2 domains of Myo5, respectively.

The second part of our two-hybrid assay (Figures 14-15) focused on studying which specific domains of Myo5 are necessary and sufficient to interact with Osh2 and Osh3. The main conclusion of these assays was that Osh2 interacts with the Myo5 SH3 domain, which was described to bind to proline-rich sequences containing a core PXXP motif (where X is any amino acid) (Sparks et al. 1994 and Simon & Schreiber 1995). To confirm this probably hypothesis, we demonstrated using a two hybrid assay that mutation of a conserve W residue within the SH3 domain that critically contributes to the interaction with polyP motifs, completely obliterated the Myo5 Osh2 interaction (Figure 16).

In the search for some proline-rich motifs within the Osh2 protein sequence, three initial candidates were found: aa 768 to 784, aa 770 to 786 and aa 1189 to 1202 (Figures 20 and 21). As the construction used for Osh2-N only bears aa 1 to 860 and the C-terminal fragment containing the ORD did not show any interaction, we would propose that the proline-rich region by which Osh2 interacts with the Myo5 SH3 domain is that comprised within aa 768 to 786.

In line with this hypothesis we observe that this polyp sequence is absent in Osh1, which does not interact with Myo5 despite having a high degree of sequence homology.

The fragment showing this region of a global Osh1 and Osh2 alignment performed using NEEDLE EMBOS is shown in figure 20.

```

OSH1          701 FIEATKESDEDSDADEFFDAEE-----AASDKKA---- 729
                ||.|||||.||.||||||:|.|          ||:.|.|
OSH2          730 FISATKEEDEASDADEFYDAAELVDEVTELTEAHPEISTAAAPKHAPPV 779
OSH1          730 -----NDSE-----DLTT----- 737
                |||:          :|.|
OSH2          780 PNETDNDSQYVQDEKSKIESNVEKTSQKFEKQNNLVTEDEPKTDQSLKNF 829

```

Figure 20: Fragment 1 of NEEDLE EMBOS Global Alignment of OSH1 and OSH2. In red (aa 768 to 784)

```

OSH1          1082 NLTSFALTNLALPPLHLPYLAPTD SRLRPDQRAMENGEYDKAAAEKHRVE 1131 ct
a              |||.||:|||||.|||:|:|.|||:|||||||:|.||:|.||.|||
w. OSH2       1177 NLTPFAITLNAPQPHLLPWLPTDTRLRPDQRAMEDGRYDEAGDEKFRVE 1226

```

Figure 21: Fragment 2 of NEEDLE EMBOS Global Alignment of OSH1 and OSH2. In blue (aa 1189 to 1202) is indicated another possible proline-rich motif of OSH2.

Finally, we analysed the Myo5 domains mediating the interaction with Osh3. The results of this assay were remarkable because they suggested that the interaction between Osh3 and Myo5 is different than the one mediating the Osh2 and Myo5 binding. In detail, the assay suggested that the Osh3-N terminal fragment interacts with pEG202MYO5, pEG202myo5-TH2cD and pEG202myo5(SH3,TH2c)D, indicating that at least part of the TH1 and TH2 domains of Myo5 are essential for the interaction with OSH3. Further experiments will be required in the future to define the particular amino acids of Osh3 and Myo5, participating in this interaction since the TH2 and TH1 domains have only been described to interact with actin and acidic phospholipids, respectively.

6. CONCLUSIONS AND FUTURE LINES

- Osh2 and probably Osh3 interact with Myo5.
- Osh1, Osh4, Osh5, Osh6 and Osh7 most probably do not directly interact with Myo5.
- Osh2 interacts with the Myo5 SH3 domain most likely via a polyP motif of Osh2 comprised within aa 768 to aa 786.
- A region included within the Myo5 TH1 and TH2 domains is the responsible for the probable interaction with the N- terminal region of Osh3.

Even though we demonstrated the interaction between Myo5 and Osh2, the functional relevance of this interaction in the context of endocytic budding still needs to be addressed. Mutating the poly-proline motif of Osh2 and the conserved W1123S of the Myo5 SH3 will provide a powerful tool to specifically disrupt the interaction between Osh2 and Myo5, minimizing secondary effects caused by deletion of larger regions of the proteins or by the complete knock outs. Nevertheless, one should take into account when interpreting the phenotypes of these mutations that the W1123S mutation of the Myo5 SH3 domain will also disrupt the interaction with Vrp1 and therefore, it will compromise the activity of the myosin-I as an NPF. In any case, even though we have probably been able of determining the Osh2 proline-rich motif responsible of the interaction, we still need to do a two-hybrid assay between the Myo5 SH3 domain and a construction entailing at the Osh2 N-terminus with a mutation in the region aa 768 to 786 and to perform immunoprecipitations with the point mutations in the endogenous proteins to demonstrate that we disrupt their binding.

Moreover, to determine the role of this protein-protein interaction in endocytosis, it would be recommendable to design a strain with both proteins tagged with different fluorescent proteins such as GFP and mCherry, to try visualizing their transient interaction *in vivo* during the endocytic event.

Analogous experiments will be conducted to define in detail the residues involved in the Myo5-Osh3 interaction and to investigate its putative role in endocytosis and in establishing the ER/endocytic sites contact sites. Preliminary results from J. Encinar in the group though suggest that the endocytic defects of *osh3Δ* mutant are less compared to those in an *osh2Δ* mutant.

Even though we proved the interaction through two-hybrid assays, we still don't know which precise domains of both proteins are the ones which physically interact. However, as the constructions that interact are OSH3-N (aa 1 – 604) and Myo5 pEG202myo5(SH3,TH2c)D (TH1 and TH2 domains), the next step could be to design smaller constructs to try to narrow down the possible interacting domains. In addition, we guess that the physical interaction is transient, but to know the time-lapse of the interaction and its function in the endocytosis pathway, we could also construct fusion proteins of Myo5 and OSH3 with fluorescent proteins.

7. REFERENCES

- Anderson, B.L. et al., 1998. The Src homology domain 3 (SH3) of a yeast type I myosin, Myo5p, binds to verprolin and is required for targeting to sites of actin polarization. *The Journal of Cell Biology*, 141(6), pp.1357–1370.
- Beh, C.T. et al., 2001. Overlapping functions of the yeast oxysterol-binding protein homologues. *Genetics*, 157(3), pp.1117–1140.
- Boettner, D.R. et al., 2012. Lessons from yeast for clathrin-mediated endocytosis. *Nature Cell Biology*, 14(1), pp.2–10.
- De Craene, J.-O. et al., 2006. Rtn1p Is Involved in Structuring the Cortical Endoplasmic Reticulum. *Molecular biology of the cell*, 17, pp.3009–3020.
- Drubin, D.G. et al., 1988. Yeast actin-binding proteins: evidence for a role in morphogenesis. *Journal of Cell Biology*, 107(6 Pt 2), pp.2551–2561.
- Engqvist-Goldstein, Å.E.Y. & Drubin, D.G., 2003. ACTIN ASSEMBLY AND ENDOCYTOSIS: From Yeast to Mammals. *Annual Review of Cell and Developmental Biology*, 19(1), pp.287–332.
- Evangelista, M. et al., 2000. A role for myosin-I in actin assembly through interactions with Vrp1p, Bee1p, and the Arp2/3 complex. *The Journal of Cell Biology*, 148(2), pp.353–362.
- Fernández-Golbano, I.M. et al., 2014. Crosstalk between PI(4,5)P2 and CK2 Modulates Actin Polymerization during Endocytic Uptake. *Developmental Cell*, 30, pp.746–758.
- Gavin, A.-C. et al., 2006. Proteome survey reveals modularity of the yeast cell machinery. *Nature*, 440, pp.631–636.
- Geli, M.I. et al., 2000. An intact SH3 domain is required for myosin I-induced actin polymerization. *The EMBO journal*, 19(16), pp.4281–4291.
- Geli, M.I. & Riezman, H., 1996. Role of type I myosins in receptor-mediated endocytosis in yeast. *Science*, 272(5261), pp.533–535.
- Geli, M.I. et al., 1998. Distinct functions of calmodulin are required for the uptake step of receptor-mediated endocytosis in yeast: The type I myosin Myo5p is one of the calmodulin targets. *EMBO Journal*, 17(3), pp.635–647.
- Ghaemmaghami, S. et al., 2003. Global analysis of protein expression in yeast. *Nature*, 425(1997), pp.737–41.
- Gietz, R.D. & Akio, S., 1988. New yeast-Escherichia coli shuttle vectors constructed with in vitro mutagenized yeast genes lacking six-base pair restriction sites. *Gene*, 74(2), pp.527–534.
- Girao, H. et al., 2008. Actin in the endocytic pathway: From yeast to mammals. *FEBS Letters*, 582, pp.2112–2119.
- Goode, B.L. et al., 2001. Activation of the Arp2/3 complex by the actin filament binding protein Abp1p. *The Journal of Cell Biology*, 153(3), pp.627–634.
- Goodson, H. V. et al., 1996. Synthetic lethality screen identifies a novel yeast myosin I gene (MYO5): Myosin I proteins are required for polarization of the actin cytoskeleton. *The Journal of Cell Biology*, 133(6), pp.1277–1291.
- Grosshans, B.L. et al., 2006. TEDS site phosphorylation of the yeast myosins I is required for ligand-induced but not for constitutive endocytosis of the G protein-coupled receptor Ste2p. *Journal of Biological Chemistry*, 281(16).
- Grötsch, H. et al., 2010. Calmodulin dissociation regulates Myo5 recruitment and function at endocytic sites. *The EMBO journal*, 29(17), pp.2899–914.
- Gyuris, J. et al., 1993. Cdi1, a human G1 and S phase protein phosphatase that associates with Cdk2. *Cell*, 75, pp.791–803.
- Hammond, G.R. V et al., 2012. PI4P and PI(4,5)P2 Are Essential But Independent Lipid Determinants of Membrane Identity. *Science*, 337, pp.727–730.
- Hasson, T. & Mooseker, M.S., 1995. Molecular motors, membrane movements and physiology: emerging roles for myosins. *Current Opinion in Cell Biology*, 7, pp.587–594.
- Hollingsworth, R. & White, J.H., 2004. Target discovery using the yeast two-hybrid system. *Drug Discovery Today*, 3(3), pp.97–103.
- Horvath, A. & Riezman, H., 1994. Rapid protein extraction from *Saccharomyces cerevisiae*. *Yeast*, 10(10), pp.1305–1310.
- Idrissi, F.-Z. et al., 2012. Ultrastructural dynamics of proteins involved in endocytic budding. *Proceedings of the National Academy of Sciences*, 109(39), pp.E2587–E2594.
- Idrissi, F.Z. et al., 2008. Distinct acto/myosin-I structures associate with endocytic profiles at the plasma membrane. *Journal of Cell Biology*, 180(6), pp.1219–1232.
- Idrissi, F.Z. & Geli, M.I., 2014. Zooming in on the molecular mechanisms of endocytic budding by time-resolved electron microscopy. *Cellular and Molecular Life Sciences*, 71, pp.641–657.

- Ito, H. et al., 1983. Transformation of intact yeast cells treated with alkali cations. *Journal of Bacteriology*, 153(1), pp.163–168.
- Kaiser, S.E. et al., 2005. Structural basis of FFAT motif-mediated ER targeting. *Structure*, 13, pp.1035–1045.
- Kukulski, W. et al., 2011. Correlated fluorescence and 3D electron microscopy with high sensitivity and spatial precision. *The Journal of Cell Biology*, 192(1), pp.111–119.
- Kulak, N.A. et al., 2014. Minimal, encapsulated proteomic-sample processing applied to copy-number estimation in eukaryotic cells. *Nature methods*, 11(3), pp.319–24.
- Kumari, S., Mg, S. & Mayor, S., 2010. Endocytosis unplugged: multiple ways to enter the cell. *Cell research*, 20, pp.256–275.
- Laemmli, U.K., 1970. Cleavage of Structural Proteins during the Assembly of the Head of Bacteriophage T4. *Nature*, 227(5259), pp.680–685.
- Lechler, T. et al., 2001. A two-tiered mechanism by which Cdc42 controls the localization and activation of an Arp2/3-activating motor complex in yeast. *The Journal of Cell Biology*, 155(2), pp.261–270.
- Lechler, T. et al., 2000. Direct involvement of yeast type I myosins in Cdc42-dependent actin polymerization. *The Journal of Cell Biology*, 148(2), pp.363–373.
- Lecuit, T. & Pilot, F., 2003. Developmental control of cell morphogenesis: a focus on membrane growth. *Nature Cell biology*, 5(2), pp.103–108.
- Levine, T.P. & Munro, S., 2001. Dual targeting of Osh1p, a yeast homologue of oxysterol-binding protein, to both the Golgi and the nucleus-vacuole junction. *Molecular biology of the cell*, 12, pp.1633–1644.
- Li, X. et al., 2002. Analysis of oxysterol binding protein homologue Kes1p function in regulation of Sec14p-dependent protein transport from the yeast Golgi complex. *The Journal of Cell Biology*, 157(1), pp.63–77.
- Loewen, C.J.R. et al., 2007. Inheritance of cortical ER in yeast is required for normal septin organization. *The Journal of Cell Biology*, 179(3), pp.467–483.
- Loewen, C.J.R. et al., 2003. A conserved ER targeting motif in three families of lipid binding proteins and in Opi1p binds VAP. *EMBO Journal*, 22(9), pp.2025–2035.
- Longtine, M.S. et al., 1998. Additional modules for versatile and economical PCR-based gene deletion and modification in *Saccharomyces cerevisiae*. *Yeast*, 14, pp.953–961.
- Manford, A.G. et al., 2012. ER-to-Plasma Membrane Tethering Proteins Regulate Cell Signaling and ER Morphology. *Developmental Cell*, 23, pp.1129–1140.
- McMahon, H.T. & Boucrot, E., 2011. Molecular mechanism and physiological functions of clathrin-mediated endocytosis. *Nature reviews. Molecular cell biology*, 12, pp.517–533.
- Merrifield, C.J., 2004. Seeing is believing: Imaging actin dynamics at single sites of endocytosis. *Trends in Cell Biology*, 14(7), pp.352–358.
- Pollard, T.D. et al., 1991. MYOSIN-I. *Annual Review of Physiology*, 53, pp.653–681.
- Prinz, W.A. et al., 2000. Mutants affecting the structure of the cortical endoplasmic reticulum in *Saccharomyces cerevisiae*. *The Journal of Cell Biology*, 150(3), pp.461–474.
- Raychaudhuri, S. & Prinz, W.A., 2010. The diverse functions of oxysterol-binding proteins. *Annual review of cell and developmental biology*, 26, pp.157–77.
- Sambrook, J. & Russell, D.W., 2012. *Molecular cloning: a laboratory manual*, 4th ed (Cold Spring Harbor, N.Y., Cold Spring Harbor Laboratory Press).
- Schulz, T.A. et al., 2009. Lipid-regulated sterol transfer between closely apposed membranes by oxysterol-binding protein homologues. *Journal of Cell Biology*, 187(6), pp.889–903.
- Scita, G. & Di Fiore, P.P., 2010. The endocytic matrix. *Nature*, 463, pp.464–473.
- Simon, J.A. & Schreiber, S.L., 1995. Grb2 SH3 binding to peptides from Sos: evaluation of a general model for SH3-ligand interactions. *Chemistry and Biology*, 2(1), pp.53–60.
- Sparks, A.B. et al., 1994. Identification and Characterization of Src SH3 Ligands from Phage-displayed Random Peptide Libraries. *The Journal of Biological Chemistry*, 269(39), pp.23853–23856.
- Stefan, C.J. et al., 2011. Osh proteins regulate phosphoinositide metabolism at ER-plasma membrane contact sites. *Cell*, 144, pp.389–401.
- Stefan, C.J. et al., 2013. ER-PM connections: Sites of information transfer and inter-organelle communication. *Current Opinion in Cell Biology*, 25, pp.434–442.
- Sun, Y., 2006. Endocytic Internalization in Budding Yeast Requires Coordinated Actin Nucleation and Myosin Motor Activity. *Developmental Cell*, 11, pp.33–46.
- Taylor, M.J., 2011. A high precision survey of the molecular dynamics of mammalian clathrin-mediated endocytosis. *PLoS Biology*, 9(3), pp.1–23.

- Tonikian, R. et al., 2009. Bayesian modeling of the yeast SH3 domain interactome predicts spatiotemporal dynamics of endocytosis proteins. *PLoS Biology*, 7(10), pp.1–20.
- Weinberg, J. & Drubin, D.G., 2012. Clathrin-mediated endocytosis in budding yeast. *Trends in Cell Biology*, 22(1), pp.1–13.
- West, M. et al., 2011. A 3D analysis of yeast ER structure reveals how ER domains are organized by membrane curvature. *The Journal of Cell Biology*, 193(2), pp.333–346.
- Winter, D., Lechler, T. & Li, R., 1999. Activation of the yeast Arp2/3 complex by Bee1p, a WASP-family protein. *Current Biology*, 9, pp.501–504.
- Wyles, J.P., McMaster, C.R. & Ridgway, N.D., 2002. Vesicle-associated membrane protein-associated protein-A (VAP-A) interacts with the oxysterol-binding protein to modify export from the endoplasmic reticulum. *The Journal of Biological Chemistry*, 277(33), pp.29908–29918.

Annex

1. Plasmids

Plasmid	Insert	Yeast characteristics: Marker /Origin	<i>E. coli</i> characteristics: Marker /Origin	Reference
pSH18-34	8LexA operator + LacZ	URA3 / 2 μ	AMP ^R / Ori	(Gyuris et al. 1993)
pEG202	LexA	HIS3 / 2 μ	AMP ^R / Ori	(Gyuris et al. 1993)
pRFHM1	LexA Prot+ Bicoid	HIS3 / 2 μ	AMP ^R / Ori	(Gyuris et al. 1993)
pJG4-5END5	GALpromotor+SV40NLS+B42+HA+END5	TRP1 / 2 μ	AMP ^R / Ori	
pEG202MYO5	LEXA + MYO5(aa757-1219)	HIS3 / 2 μ	AMP ^R / Ori	(Geli et al. 2000)
pEG202myo5-TH2cD	LEXA + MYO5(aa757-1181)	HIS3 / 2 μ	AMP ^R / Ori	(Geli et al. 2000)
pEG202myo5(SH3,TH2c)D	LEXA + MYO5(aa757-1091)	HIS3 / 2 μ	AMP ^R / Ori	(Geli et al. 2000)
pEG202-myo5-(TH2,SH3)D	LEXA + MYO5(aa757-996)	HIS3 / 2 μ	AMP ^R / Ori	(Geli et al. 2000)
pEG202(TH2,SH3)	LEXA + MYO5(aa984-1219)	HIS3 / 2 μ	AMP ^R / Ori	(Geli et al. 2000)
pEG202(SH3,TH2c)	LEXA + MYO5(aa1085-1219)	HIS3 / 2 μ	AMP ^R / Ori	(Geli et al. 2000)
pEG202(SH3*,TH2c)	LEXA+MYO5(aa1085-1220) mutated W1123S	HIS3 / 2 μ	AMP ^R / Ori	(Geli et al. 2000)
pEG202(TH2c)	LEXA + MYO5(aa1142-1219)	HIS3 / 2 μ	AMP ^R / Ori	(Geli et al. 2000)
pEG202(TH2n)	LEXA + MYO5(aa984-1091)	HIS3 / 2 μ	AMP ^R / Ori	(Geli et al. 2000)
pEG202(SH3)	LEXA + MYO5(aa1085-1181)	HIS3 / 2 μ	AMP ^R / Ori	(Geli et al. 2000)
pJG4-5	GAL1 promotor-SV40NLS-B42-HA	TRP1 / 2 μ	AMP ^R / Ori	(Gyuris et al. 1993)
pJG4-5OSH1	OSH1	TRP1 / 2 μ	AMP ^R / Ori	
pJG4-5OSH2-N	OSH2-N (aa1-860)	TRP1 / 2 μ	AMP ^R / Ori	
pJG4-5OSH2-C	OSH2-C (aa840-1240)	TRP1 / 2 μ	AMP ^R / Ori	
pJG4-5OSH3-N	OSH3-N (aa1-604)	TRP1 / 2 μ	AMP ^R / Ori	
pJG4-5OSH3-N	OSH3-C (aa605-997)	TRP1 / 2 μ	AMP ^R / Ori	
pJG4-5OSH4	OSH4	TRP1 / 2 μ	AMP ^R / Ori	
pJG4-5OSH5	OSH5	TRP1 / 2 μ	AMP ^R / Ori	
pJG4-5OSH6	OSH6	TRP1 / 2 μ	AMP ^R / Ori	
pJG4-5OSH7	OSH7	TRP1 / 2 μ	AMP ^R / Ori	

Plasmid	Insert	Yeast characteristics: Marker /Origin	<i>E. coli</i> characteristics: Marker /Origin	Reference
pFA6A-3HA-HIS3MX6	3HA-HIS3MX6	HIS5 / 2 μ	AMP ^R / Ori	(Longtine et al. 1998)
p33ProtA-MYO5	2protA-TEV-MYO5	URA3 / CEN4	AMP ^R / Ori	

Table 7: Plasmids used for immunoprecipitation experiments

Strain	Genotype	Source
EGY48 pSH 14-38	MAT α trp1 his3 ura3 6LexAop-LEU2 + pSH18-38	R. Brent

2. Yeast strains

Table 8: Basic strain for the Two Hybrid experiments

Strain	Plasmid 1	Plasmid 2	Strain	Plasmid 1	Plasmid 2
1	pJG4-5	pEG202MYO5	18	215	pEG202-myo5-(TH2,SH3)D
2	pJG4-5	pEG202(TH2,S H3)	19	215	pEG202(TH2n)
3	pJG4-5	pEG202(SH3,T H2c)	20	215	pEG202(SH3)
4	pJG4-5	pEG202(TH2c)	21	215	pRFHM1
5	pJG4-5	pEG202myo5-TH2cD	22	215	428
6	pJG4-5	pEG202myo5(S H3,TH2c)D	23	pJG4-5OSH1	pEG202MYO5
7	pJG4-5	pEG202-myo5-(TH2,SH3)D	24	pJG4-5OSH1	pEG202(TH2,S H3)
8	pJG4-5	pEG202(TH2n)	25	pJG4-5OSH1	pRFHM1
9	pJG4-5	pEG202(SH3)	26	pJG4-5OSH2-N	pEG202MYO5
10	pJG4-5	pRFHM1	27	pJG4-5OSH2-N	pEG202(TH2,S H3)
11	pJG4-5	pEG202(SH3*,T H2c)	28	pJG4-5OSH2-N	pEG202(SH3,T H2c)
12	pJG4-5END5	pEG202MYO5	29	pJG4-5OSH2-N	pEG202(TH2c)

Table 6: Plasmids used for Two Hybrid experiments.

13	pJG4-5END5	pEG202(TH2,S H3)	30	pJG4-5OSH2-N	pEG202myo5-TH2cD
14	pJG4-5END5	pEG202(SH3,T H2c)	31	pJG4-5OSH2-N	pEG202myo5(S H3,TH2c)D

Strain	Plasmid 1	Plasmid 2	Strain	Plasmid 1	Plasmid 2
		H2c)			
15	pJG4-5END5	pEG202(TH2c)	32	pJG4-5OSH2-N	pEG202-myo5-(TH2,SH3)D
16	pJG4-5END5	pEG202myo5-TH2cD	33	pJG4-5OSH2-N	pEG202(TH2n)
17	pJG4-5END5	pEG202myo5(SH3,TH2c)D	34	pJG4-5OSH2-N	pEG202(SH3)
35	pJG4-5OSH2-N	pRFHM1	50	pJG4-5OSH3-N	pEG202MYO5
36	pJG4-5OSH2-N	pEG202(SH3*,TH2c)	51	pJG4-5OSH3-N	pEG202(TH2,SH3)
37	pJG4-5OSH2-C	pEG202MYO5	52	pJG4-5OSH3-N	pRFHM1
38	pJG4-5OSH2-C	pEG202(TH2,SH3)	53	pJG4-5OSH4	pEG202MYO5
39	pJG4-5OSH2-C	pRFHM1	54	pJG4-5OSH4	pEG202(TH2,SH3)
40	pJG4-5OSH3-N	pEG202MYO5	55	pJG4-5OSH4	pRFHM1
41	pJG4-5OSH3-N	pEG202(TH2,SH3)	56	pJG4-5OSH5	pEG202MYO5
42	pJG4-5OSH3-N	pEG202(SH3,TH2c)	57	pJG4-5OSH5	pEG202(TH2,SH3)
43	pJG4-5OSH3-N	pEG202(TH2c)	58	pJG4-5OSH5	pRFHM1
44	pJG4-5OSH3-N	pEG202myo5-TH2cD	59	pJG4-5OSH6	pEG202MYO5
45	pJG4-5OSH3-N	pEG202myo5(SH3,TH2c)D	60	pJG4-5OSH6	pEG202(TH2,SH3)
46	pJG4-5OSH3-N	pEG202-myo5-(TH2,SH3)D	61	pJG4-5OSH6	pRFHM1
47	pJG4-5OSH3-N	pEG202(TH2n)	62	pJG4-5OSH7	pEG202MYO5
48	pJG4-5OSH3-N	pEG202(SH3)	63	pJG4-5OSH7	pEG202(TH2,SH3)
49	pJG4-5OSH3-N	pRFHM1	64	pJG4-5OSH7	pRFHM1

Table 8: Strains generated by episomal plasmid introduction used for the Two Hybrid experiments

Strain	Genotype	Source
SCMIG136	<i>Matalpha his3 leu2 lys2 ura3 myo5D::KMX (yhr109w::KMX)</i>	
SCMIG1201	<i>Matalpha his3 leu2 lys2 ura3 myo5D::KMX (yhr109w::KMX) OSH1-3HA:HIS3MX</i>	This study
SCMIG1202	<i>Matalpha his3 leu2 lys2 ura3 myo5D::KMX (yhr109w::KMX) OSH2-3HA:HIS3MX</i>	This study
SCMIG1203	<i>Matalpha his3 leu2 lys2 ura3 myo5D::KMX (yhr109w::KMX) OSH3-3HA:HIS3MX</i>	This study
SCMIG1204	<i>Matalpha his3 leu2 lys2 ura3 myo5D::KMX (yhr109w::KMX) OSH4-3HA:HIS3MX</i>	This study
SCMIG1205	<i>Matalpha his3 leu2 lys2 ura3 myo5D::KMX (yhr109w::KMX) OSH5-3HA:HIS3MX</i>	This study
SCMIG1206	<i>Matalpha his3 leu2 lys2 ura3 myo5D::KMX (yhr109w::KMX) OSH6-3HA:HIS3MX</i>	This study
SCMIG1207	<i>Matalpha his3 leu2 lys2 ura3 myo5D::KMX (yhr109w::KMX) OSH7-3HA:HIS3MX</i>	This study
SCMIG1208	<i>Matalpha his3 leu2 lys2 ura3 myo5D::KMX (yhr109w::KMX) + p33ProtA-MYO5</i>	This study

Strain	Genotype	Source
SCMIG1209	<i>Matalpha his3 leu2 lys2 ura3 myo5D::KMX (yhr109w::KMX) OSH2-3HA:HIS3MX + p33ProtA-MYO5</i>	This study
SCMIG1210	<i>Matalpha his3 leu2 lys2 ura3 myo5D::KMX (yhr109w::KMX) OSH3-3HA:HIS3 + p33ProtA-MYO5</i>	This study

Table 9: Strains generated by homologous recombination used for the immunoprecipitation experiments

3. Global Alignment NEEDLE EMBOSS between OSH2 and OSH3 protein sequences

```

Aligned_sequences: 2
# 1: OSH1
# 2: OSH2
# Matrix: EBLOSUM62
# Gap_penalty: 10.0
# Extend_penalty: 0.5
#
# Length: 1308
# Identity: 651/1308 (49.8%)
# Similarity: 867/1308 (66.3%)
# Gaps: 143/1308 (10.9%)
# Score: 3243.5

```

```

OSH1      1 MEQPDLSVV----AISKPLKLLKLLDALRQGSFPNLQDLLKKQFQPLDDP      46
           |.:.||||..  .:|||||:|:|:|.|.|.|.|.|.|.|.|.|.|.|.|.
OSH2      1 MSREDLSIAEDLNQVSKPLLVKLLLEVLGQDFKHLKALVDNEFQPKDDP      50

OSH1     47 NVQQVLHMLHYAVQVAPMAVIKEIVHHWV-----STTNTTFLNIHLDL      90
           :|||||:|:|:|:|:|:|:|:|:|:|:|:|:|:|:|:|:|:|:|:|:|:|:|:|
OSH2     51 SVQQVLNLIHLYAVQVAPILLIKEIVAHWVDQVGDEKSSSKSDDGIHLDL     100

OSH1     91 NERDSNGNTPLHIAAYQSRGDIVAFLLDQPTINDCVLNNSHLQAIEMCKN     140
           |.:.|.|||||:|:|:|:|:|:|:|:|:|:|:|:|:|:|:|:|:|:|:|:|:|:|
OSH2    101 NYQDENGNTPLHLAAAQSRSDVISFLLSQKSINDCVKNKAHQQLDMCKD     150

OSH1    141 LNIAQMMQVKRSTYVAETAQEFRTAFNNRDFGHLESILSSPRNAELLDIN     190
           ||:|:|:|:|:|:|:|:|:|:|:|:|:|:|:|:|:|:|:|:|:|:|:|:|
OSH2    151 LNVAQMIQLKRDDYFLETVHSLRAAMNKRDFSKLDSIWKNPRNLNLLDIN     200

OSH1    191 GMDPETGDTVLEHFVKKRDVIMCRWLLLEHGADPFKRDGKGLPIELVRKV     240
           |:|:|:|:|:|:|:|:|:|:|:|:|:|:|:|:|:|:|:|:|:|:|:|:|:|:|
OSH2    201 GIDPETGTTLLYEYSQKKDIEMCQWLLKHGAEATVKDGGKGRSPLDLVKNI     250

OSH1    241 NENDTATNTKIAIDIELKKLLERATREQSVI--DVTNNNLHEAPTYKGYL     288
           .....| .:..:|:|:|:|:|:|:|:|:|:|:|:|:|:|:|:|:|:|:|
OSH2    251 KLPKPSN-NVTPEIKLKNLLEKNLREQAIVHEDVASS---KPPTYKGF      296

OSH1    289 KKWTNFAQGYKLRWFILSSDGKLSYYIDQADTKNACRGSLSMSSCSLHLD     338
           |||:|:|:|:|:|:|:|:|:|:|:|:|:|:|:|:|:|:|:|:|:|:|:|:|
OSH2    297 KKWTNFAHGYKLRWFILSGDGNLSYKQSHVDRP-RGTLKVSTCRRLHID     345

OSH1    339 SSEKLFKEIIGNGNVIRWHLKGNHPIETNRWVWAIQGAIRYAKDREILL     388
           |||:|:|:|:|:|:|:|:|:|:|:|:|:|:|:|:|:|:|:|:|:|:|:|:|
OSH2    346 SSEKLNPELLGGITGTTRWRLKGNHPIETTRWVWAIQSAIRFAKDKIELN     395

OSH1    389 HNGPYSPSLALSHGLSSKVS-----NKENLHATSKR      419
           .....|||:|:|:|:|:|:|:|:|:|:|:|:|:|:|:|:|:|:|:|
OSH2    396 KKKAVPPSLALKNKSPALISHSKTQGSQYYQHTLHKEVIQPSV      445

```


OSH2 1227 EKQRAARRKREENNLEYHPQWFVRDTHPITKAKYWRYTGKYWVKRRDHDL 1276
 OSH1 1pJG4-5 KDCADIF* 1189
 | | | . | | |
 OSH2 1277 KDCGDIF* 1284

4. SDS-PAGE gels composition

All SDS-PAGE gels used for this project contained 10% of polyacrylamide. See table 10 for the composition.

	STACKING	RESOLVING
H₂O	1800 µl	5000 µl
Buffer	700 µl	2500 µl
40% Acrylamide	300 µl	2500 µl
10% APS	18 µl	90 µl
TEMED	6 µl	9 µl

Table 10: SDS-PAGE 10% polyacrylamide gels. H₂O = dd water. Stacking buffer = 500 mM Tris Base, 0.4 % SDS, ph= 6,8. Resolving buffer = 1,5 M Tris Base, 0.4 % SDS, ph= 8,8. 40 % Acrylamide : N N' Methylbisacrylamide (37.5:1) (Fluka 396401). 10% APS = 0.5 gr of Amonium Persulfate (Fluka 09913). TEMED = NNN'N' Tetramethylethylenediamine (Fluka 07007)